



## MRM methods for high precision shift measurements in H/DX-MS

Andrew J. Percy<sup>a</sup>, David C. Schriemer<sup>a,b,\*</sup>

<sup>a</sup> Department of Chemistry, University of Calgary, Canada

<sup>b</sup> Department of Biochemistry and Molecular Biology, University of Calgary, Canada

### ARTICLE INFO

#### Article history:

Received 29 May 2010

Received in revised form 5 July 2010

Accepted 7 July 2010

Available online 15 July 2010

#### Keywords:

H/DX

Multiple reaction monitoring

Mass shift perturbation

Simulations

### ABSTRACT

Conventional methods for the measurement of deuterium exchange data suffer limitations arising from extensive deuteration protocols, MS domain data collection and short chromatographic run times. Together, these limitations create complex spectra with reduced dynamic range and the potential for significant spectral overlap. For applications of mass shift perturbation detection, we present an improved method for targeting sequence coverage, based upon multiple reaction monitoring (MRM) on a triple quadrupole platform. Two classes of MRM detection are described and validated, each requiring only two transitions per peptide. These methods were developed through simulations of MRM sampling of isotopic distributions, and validated by shift measurements for a range of peptides. An MRM method involving resolved offset transmission windows in Q1 and a fixed window in Q3 provides a generic and sensitive approach. Shift measurement precision by MRM is demonstrated to match that of conventional high resolution determinations (~5% RSD) and exceed the dynamic range by over two orders of magnitude in concentration. Optimized MRM methods were applied to a set of peptides selected to discriminate between two different classes of antimetabolic drugs binding to  $\alpha/\beta$ -tubulin. The precision of the MRM methods is comparable with higher resolution conventional methods, and additionally simplify data analysis. A set of guidelines is presented to facilitate rapid development of MRM shift assays for any peptides arising from H/DX workflows.

Crown Copyright © 2010 Published by Elsevier B.V. All rights reserved.

### 1. Introduction

Hydrogen/deuterium exchange mechanisms provide significant opportunities to probe the structure-function properties of proteins and protein systems. Typical applications of the approach have involved systems of limited complexity, due in part from restrictions of the technologies applied to the measurement of the H/D exchange rate (e.g., NMR [1,2]). Mass spectrometry has permitted impressive extensions [3], but there remains significant unrealized potential to extend the scope of “bottom-up” exchange measurements towards low abundance, complex protein mixtures.

Most practical applications of the H/D methods are relational, where differences in exchange rates or levels are correlated with the structural or dynamical properties of a perturbed system. For example, H/D exchange is used extensively to characterize the

topologies of molecular interactions and to discover the allosteric effects of interactions [4–6]. Here, the mass shift is of primary importance, rather than a detailed description of the deuterium distribution. When considered from this perspective, methods should be developed that offer the highest sensitivity to changes in the isotopic mass shifts resulting from deuteration. This may be referred to as mass shift perturbation (MSP) analysis [7], because of strong similarities to an NMR technique used for similar purposes. Chemical shift perturbation (CSP) is a common method used to map binding interfaces and allosteric effects of interactions [8,9]. The fundamental shifts in both CSP and MSP bear a complex relationship to structure and dynamics. For most practical applications, the primary value of CSP or MSP measurements is to provide a statistical measure of change. That is, detecting shift perturbations that are significantly above some measure of noise in the shift provides the indication of a meaningful structure/function perturbation. This is particularly true for current bottom-up methods for shift detection, where deuterium exchange kinetics are governed by a blend of factors such as peptide length, composition, underlying structure and the relative importance of local and/or global unfolding dynamics [10–12].

Precise shift measurements for bottom-up strategies benefit from the application of high resolution mass spectrometers fronted by high resolution chromatography. These enable the detection of well-resolved isotopic distributions and comprehensive pro-

*Abbreviations:* H/DX, hydrogen/deuterium exchange; NMR, nuclear magnetic resonance; CSP, chemical shift perturbation; MSP, mass shift perturbation; MRM, multiple reaction monitoring; DMSO, dimethyl sulfoxide; K-PIPES, potassium 1,4-piperazinediethanesulfonate; GTP, guanosine 5'-triphosphate; RSD, relative standard deviation; Th, Thomson.

\* Corresponding author at: University of Calgary, Faculty of Medicine, 3330 Hospital Dr. NW, Calgary, Alberta, Canada T2N 4N1. Tel.: +1 403 210 3811; fax: +1 403 283 8727.

E-mail address: [dschriem@ucalgary.ca](mailto:dschriem@ucalgary.ca) (D.C. Schriemer).

tein sequence coverage. However, the performance gains that are realized by high resolution are always challenged by shortening the overall analysis time, to ensure that the effects of residue-specific back exchange are minimized [13,14]. This leads to practical restrictions in molecular weight of proteins amenable to the method. Recently, improvements in shift measurements for structure-function analysis have been explored through the use of isotope depletion [15], reduced labeling [16] and tandem mass spectrometry [17]. For example, we have demonstrated that labeling with lower fractional amounts of D<sub>2</sub>O can actually improve the precision of shift measurements, leading to several simplifications in the analytical workflow.

In this study, we describe a sensitive new approach to shift measurements involving H/D exchange methods, using multiple reaction monitoring (MRM) on a triple quadrupole platform. This new approach can target the sequence coverage of conventional bottom-up H/DX-MS applications and permit the interrogation of protein systems with increased complexity. It also has the potential to shorten analysis times for many applications. Two classes of MRM methods are proposed for monitoring shifts in the isotopic distributions of peptides and evaluated using simulations and experimental data, derived from both simple and complex peptide mixtures. We propose a set of optimization guidelines to promote an effective use of MRM methods for shift measurements. We demonstrate that an optimized MRM approach extends the dynamic range of shift measurements to greater than four orders of magnitude in concentration while preserving a measurement precision normally encountered in high resolution settings.

## 2. Theory and calculations

### 2.1. MRM methods for tracking mass shifts in isotopic envelopes

The mass shifts induced by H/D exchange events are typically measured by determining the centroid masses of a given peptide ion under two or more states. Measuring these mass shifts are usually associated with high resolution instruments providing resolved isotopic envelopes, but Fig. 1 suggests two methods by which MRM on a low resolution platform could be implemented.

Method 1 involves fixing an ion transmission window in Q1 and offsetting two transmission windows in Q3 by a certain amount, for a given fragment ion. It is the deuteration state of the fragment that is measured in this case. That is, as deuteration of the precursor increases within the fixed transmission window, intensity would shift out of M<sub>2</sub> and into M<sub>2</sub>+x. A minimum of two transitions are therefore required to monitor one peptide. Method 2 fixes transmission on the fragment ion in Q3, but applies two offset transmission windows in Q1. In this method the precursor ion is retained as the deuteration reporter. As deuteration shifts the distribution of the precursor ion, intensity would shift out of M<sub>1</sub> and into M<sub>1</sub>+x. A minimum of two transitions are also required for each peptide using this method.

### 2.2. Simulation methods

To test the sensitivity of these methods to mass shift perturbations, simulations were based upon neurotensin as a model peptide (sequence pyroGLYGNKPRRPYL), detected as an [M+3H]<sup>3+</sup> ion. The native distribution was modeled based solely upon <sup>13</sup>C content, and convoluted with deuteration based upon simple binomial expansions involving variable fractional D incorporation and 10 amide exchangers. Ion selection windows were modeled as modified Gaussian distributions, to simulate the conventional selections of “high”, “unit” and “low” resolution. That is, high resolution selection was modeled as a Gaussian centered upon the specified *m/z*,

with a variance of 0.014 Thomson (Th, 2% transmission on M+1 of the 3+ ion). Unit resolution was modeled as a Gaussian centered upon the specified *m/z* with a variance of 0.22 Th (10% transmission on M+3 of the 3+ ion). Low resolution was modeled as a flat-topped Gaussian opening asymmetrically to the high *m/z* side (with 10% transmission on M+6 of the 3+ ion). These are reasonable transmission window functions for a quadrupole [18]. For simulations involving fragment ions, window functions were preserved but scaled with the *m/z* (i.e., windows compressed at lower *m/z* values). All isotopic peaks were modeled as simple impulse functions spaced 1/3 Th apart. Ion selection windows were shifted as needed, in units of *x*/3 where *x* is an integer referring to the peak number from the monoisotopic ion.

To accurately reflect the isotopic composition of the peptide fragments generated in the collision cell, the <sup>13</sup>C and D content of the mass-filtered precursor ion required calculation. This cannot be assumed to be equivalent to the unfiltered precursor ion. Truncation of the envelope occurs and the size of the Q1 transmission window dictates the degree of truncation. To model this, the precursor ion isotopic distribution can be recognized as a convolution of underlying deuteration states (D = 1, 2, 3, ...) reflecting successive 1 Da shifts of the <sup>13</sup>C distribution of the native peptide. The weighting of states can be determined using multiple linear regression. Window-truncated distributions were therefore fit with window-truncated deuteration states, with the nature of the truncation determined by the window models discussed above for the three resolution settings. In this fashion, both the <sup>13</sup>C and the D content of the precursor ion passed to the collision cell could be determined over a range of deuterium incorporation. This in turn supported a modeling of any given fragment's isotopic distribution through simple binomial expansions, based upon an assessment of the number of carbons and the number of labile hydrogens. This approach allowed us to simulate, for the two possible MRM strategies, the effect of window size and placement on the mass shifts (Fig. 1).

## 3. Materials and methods

### 3.1. LC/MS

Two electrospray-based systems were used in this study. For conventional higher resolution measurements, the LC-MS configuration consisted of a prototype splitless chilled chromatography system (described previously [19]) and a QSTAR Pulsar *i* quadrupole time-of-flight (QqTOF) (AB/Sciex, Foster City, CA). Lower resolution conventional experiments and MRM measurements were performed on either a QTRAP 2000 or QTRAP 4000 hybrid triple quadrupole linear ion trap mass spectrometer (AB/Sciex, Foster City, CA). The MS systems were fitted and operated with turbo-ion spray sources and were operated in positive ion mode at 4.5 kV, at a column flow rate of 4 μl/min, with nebulization. Self-packed C<sub>18</sub> reversed-phase HPLC columns (5.5 cm × 200 μm i.d., 5 μm particles) were used for peptide separation, using a conventional acidified acetonitrile gradient.

For the analysis of α/β-tubulin protein digests, peptides were sequenced on the QSTAR as previously described [6,19] and indexed to the LC-MS dataset, capturing sequence, *m/z*, charge state and retention time information. Corresponding fragment ion spectra were obtained in enhanced product ion mode on the QTRAP at a scan rate of 1000 Da/s from 100 to 1400 Da (collision energy of 35 ± 5 eV). Candidate transitions for MRM operation were selected from the most intense primary sequence ions (*b* or *y*) for a subset of digest peptides. Under MRM analysis, the collision energy was optimized for each transition to maximize S/N and an integration time of 100 ms was employed for each transition. These conditions were

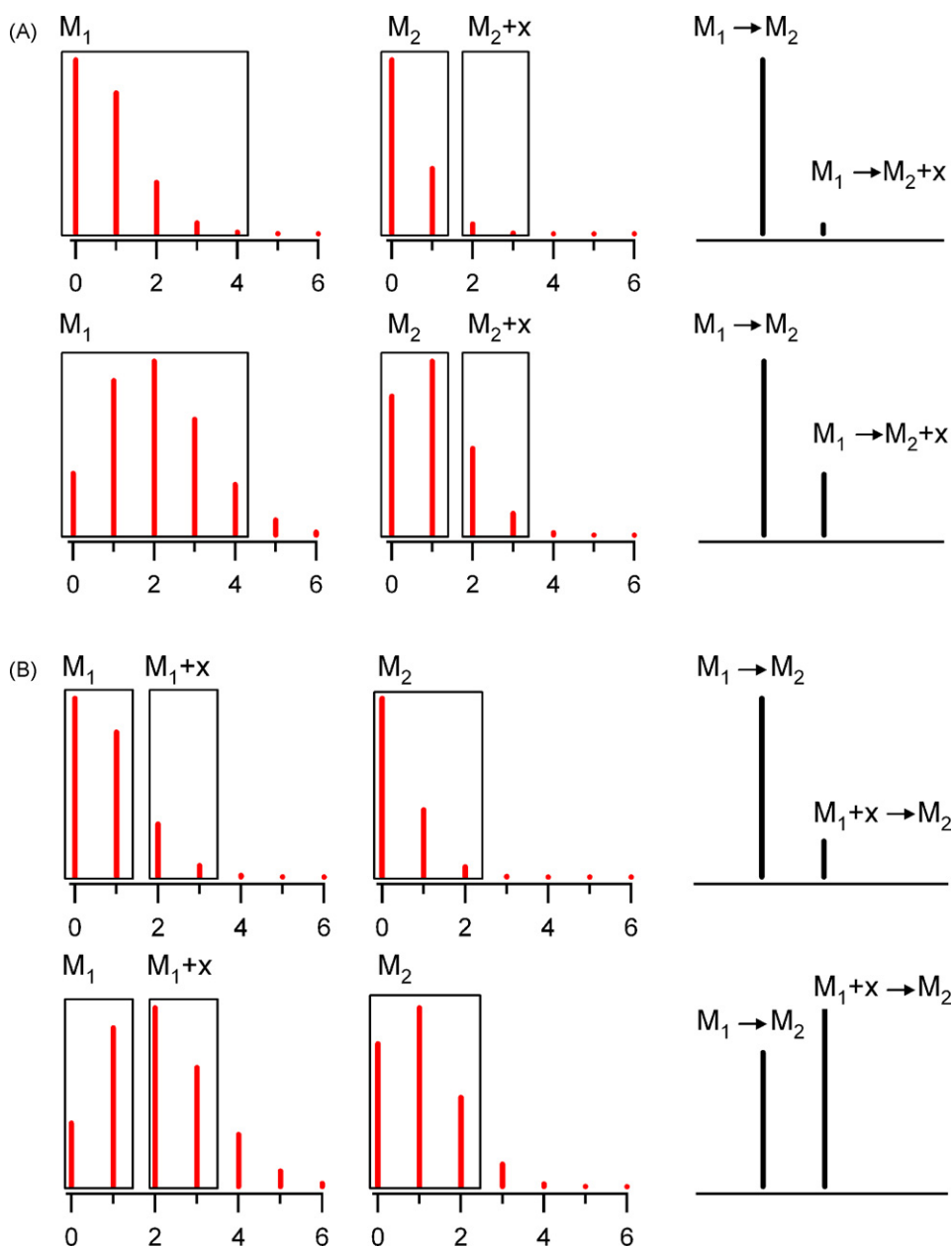


**Fig. 1.** Two possible MRM methods for sensing mass shifts in deuteration experiments. (A) Method 1, where a fundamental transition for a peptide ion is duplicated with an offset in Q3. Top panel represents a low deuteration state, and bottom panel a high deuteration state. (B) Method 2, where a fundamental transition for a peptide ion is duplicated with an offset in Q1. Top panel represents a low deuteration state, and bottom panel a high deuteration state. Here,  $x$  represents a variable window offset, with  $M_1$  and  $M_2$  the monoisotopic  $m/z$  of the precursor and fragment ions, respectively.

then applied to the two MRM methods (Fig. 1), varying the resolution of ion selection and the window offset as described below. This approach was followed for the analysis of neurotensin as well, based upon the fragment spectrum of the 3+ ion. High and unit resolutions were as defined based on default calibration routines and low resolution was defined with an offset of 0.1 in the resolution table, relative to unit resolution.

### 3.2. Sample preparation and deuterium labeling

To monitor the sensitivity of the MRM-based methods for shift detection, samples were equilibrated in solutions containing  $D_2O$  over a concentration range. Neurotensin, equilibrated in 0–25%  $D_2O$ , was directly injected into the LC/MS systems as described. The  $\alpha/\beta$ -tubulin protein dimer was digested by adding unlabeled or 20%  $D_2O$ -labeled aliquot to a slurry of immobilized pepsin in

0 or 20%  $D_2O$  digestion buffer, respectively. Digestion buffer consisted of 0.1 M glycine-HCl (pH 2.3). The  $D_2O$  present in the digest slurry permitted an equilibrated deuteration level for the tubulin samples, which allowed us to store them for subsequent experiments. Approximately 5 pmol of digest was loaded per experiment, in triplicate.

For the drug-tubulin interaction assay, the above protocol was amended as follows. Sample buffer, consisting of 1 mM guanosine 5'-triphosphate (GTP), 100 mM KCl, 1 mM  $MgCl_2$  and 10 mM potassium 1,4-piperazinediethanesulfonate (K-PIPES, pH 6.9), was used to establish  $\alpha/\beta$ -tubulin solutions with a protein concentration of 50  $\mu M$ . Prior to  $D_2O$  labeling, the tubulin solution was combined with either docetaxel, vinblastine, or a dimethylsulfoxide (DMSO) blank and incubated at 37 °C for 30 min. The final concentrations of tubulin, drug, and DMSO were 5  $\mu M$ , 40  $\mu M$ , and 4%, respectively. The dimer control lacked only the drug. After incubation, sample

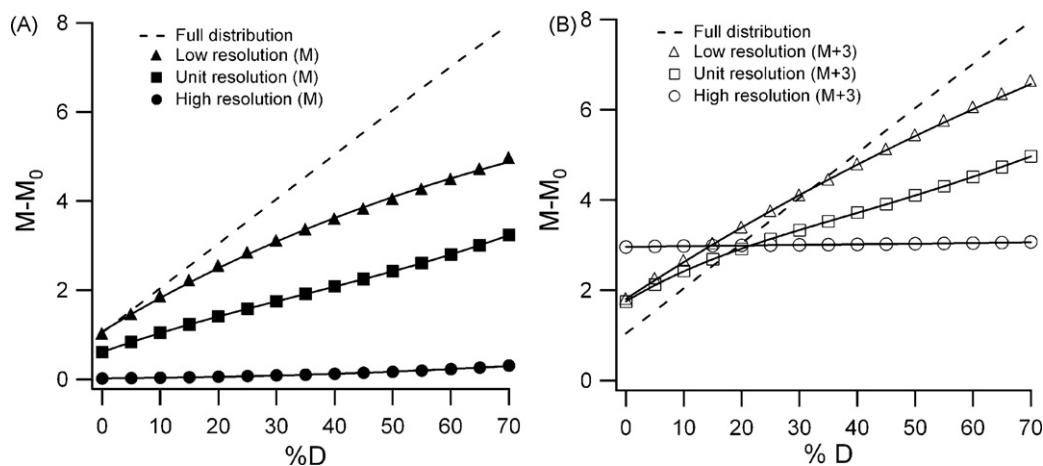


**Fig. 2.** Simulated effect of transmission window size and placement on centroid mass measurements. (A) Effect of transmission windows of variable size (low, unit, high) on the centroid mass difference as a function of %D incorporated. Transmission centered upon the monoisotopic ion of neurotensin (3+ charge state). Values referenced to the monoisotopic mass. (B) As in A, but with windows offset by 1 Th. Dashed lines represent the expected (unperturbed) centroid mass.

temperature was reduced to 20 °C for 1 min and the protein was labeled with the addition of 20% D<sub>2</sub>O at this temperature, incubated for 4 min. Pepsin digestion was performed at 0 °C for 2.5 min. All deuteration measurements were made in triplicate (from incubation to detection) and the order of runs randomized to minimize the introduction of systematic error.

### 3.3. Data analysis

Mass shift data from the QSTAR runs were exported to Hydra [20] for processing, focusing on a subset of peptides arising from the tubulin digests. Isotopic peak selection for the calculation of all centroid masses was based on the first three peaks of the isotopic envelope, using strategies described earlier [16]. Deuteration levels were determined by subtracting the centroid mass of the non-deuterated isotopic envelope from the deuterated centroid mass. Mass shifts were quantitated for the tubulin–vinblastine interaction, the microtubule–docetaxel interaction and the free-dimer control. The subset of peptides monitored represent regions of the protein that encompass the drug binding sites, the intradimer interface of  $\alpha/\beta$ -tubulin, and the interdimer interface that is formed exclusively upon docetaxel-induced microtubule assembly.

MRM data were reported as fractional transition intensities calculated from the peak area of the extracted ion chromatograms (XICs). The fractional transition intensity is defined as  $B/(A+B)$ , where  $A$  represents the lower mass transition and  $B$  the higher mass transition for each of the two methods.

### 3.4. Chemicals and reagents

All reagents were purchased from Sigma–Aldrich (St. Louis, MO, USA) with the following exceptions: formic acid (FA, 98%) was acquired from Fluka (Buchs, Switzerland), glycine (99.7%) from GE Healthcare (Uppsala, Sweden) and GTP from Roche Diagnostics (Mannheim, Germany). Immobilized pepsin was obtained from Pierce (Rockford, IL, USA) and C<sub>18</sub> beads (Magic 200 Å porosity, 5  $\mu$ m diameter) were purchased from Michrom Bioresources (Auburn, CA, USA). Purified bovine brain tubulin (cat. no. TL238-A, lot no. 781) was obtained from Cytoskeleton Inc. (Denver, CO, USA). Vinblastine was a gift from Dr. Dan L. Sackett (Laboratory of Integrative and Medical Biophysics, National Institute of Child Health and Human Development, Bethesda, MD, USA). All solvents were obtained from Fisher Scientific (Fair Lawn, NJ, USA).

## 4. Results and discussion

### 4.1. Simulations

Ion selection windows in a quadrupole filtering experiment represent an analog “integrator”. That is, upon definition of the window waveform and its dimensions, the detection event represents the summation of all ion current transmitted through this window. The resulting intensity is attributed to the  $m/z$  value specified for the window. In conventional quadrupole operation, this window is small and scanned over the  $m/z$  range of interest to generate the mass spectrum. In MRM methods, windows of user-controlled dimensions are specified in both Q1 and Q3 and integration time is maximized for an optimum S/N. In designing an MRM method for shift measurement, we first considered the effect of the window function on the fidelity of the isotopic distribution (Fig. 2).

In this figure, the isotopic distribution of neurotensin was expanded as a function of percent deuterium incorporation and the window waveforms applied. It illustrates the effect of transmission window characteristics on the centroid  $m/z$  of the ion packet transmitted to the collision cell of a triple quadrupole instrument. Obviously, none of the three conventional resolution settings faithfully transmit the entire distribution. However, “low” resolution transmission minimally distorts the distribution at low %D incorporation (<20%). At higher % incorporation, the slope diminishes as the distribution shifts away from the fixed transmission window. The transmitted ion current also diminishes with increasing deuterium in this regime. This skewing of the full distribution and the corresponding reduction in ion current becomes worse with “unit” resolution transmission. High resolution transmission obviously has a slope of zero since only one isotopic peak is selected. The simulation was repeated with a window shift of 1 Th (three isotopic peaks for this charge state). The overall response is a shift to the transmission of an ion packet bearing a higher centroid average—less noticeable with low resolution transmission but present in all cases. We therefore conclude that conventional transmission settings permit good control over the sampling of a deuterated isotopic distribution, provided that isotopic expansion is restrained to reasonable deuteration levels. As we have shown previously, this requirement does not diminish sensitivity in conventional shift measurements and therefore is not expected to be a limitation in any MRM [16]. Reduced labeling in this context allows for straightforward design of MRM transitions, as these can be developed around the monoisotopic ions of precursors and fragments.

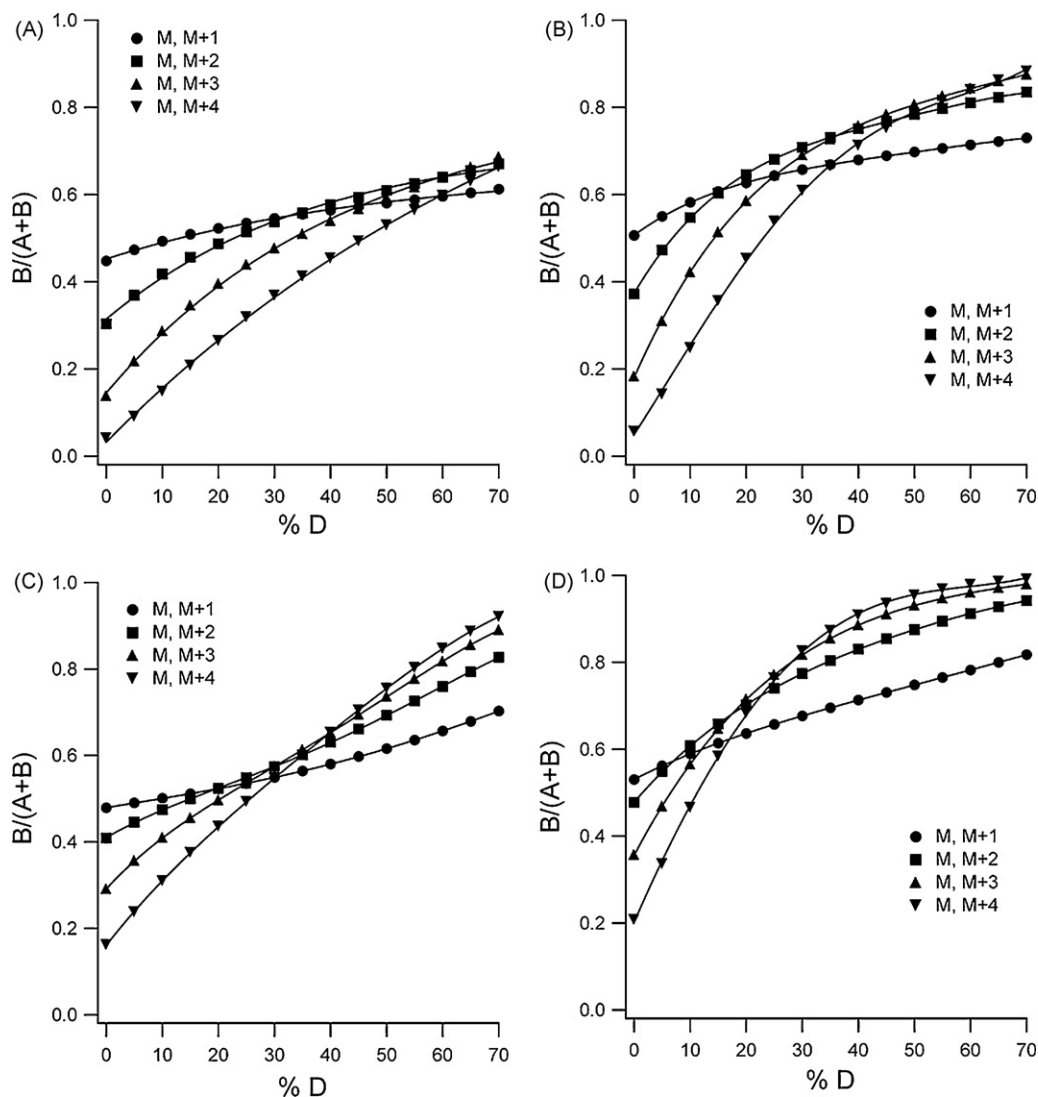


**Fig. 3.** Simulation of fractional transition intensities applied to neurotensin. (A) Method 1 was implemented with low resolution selection on  $m/z$  558 in Q1, and low resolution selection on  $M^{2+}$  ( $m/z$  643) and  $[M+x]^{2+}$  in Q3. (B) As in A, but with unit resolution in Q3 windows. (C) Method 2 was implemented with low resolution selection in Q1 on  $M^{3+}$  ( $m/z$  558) and  $[M+x]^{3+}$ , and low resolution on  $m/z$  197 in Q3. (D) As in C, but with unit resolution selection in Q1.

The simulations were then extended to evaluate the two methods of shift measurement by MRM (Fig. 1). In Method 1, Q1 is fixed at a given  $m/z$  but Q3 is toggled between two offset  $m/z$  values representing the same fragment ion. Here, deuteriation of the fragment is measured in place of the precursor ion. We evaluated the size of the offset, as well as the effect of window resolution, on shift measurement (Fig. 3A and B). The simulations demonstrate that larger offsets favor increased sensitivity to shift perturbation. This is seen in the increased slopes as a function of %D incorporated. Selecting the M and M+x masses in Q3 with higher resolution also led to increased shift sensitivity (Fig. 3B). Overall, Method 1 appears most effective when implemented with low resolution transmission of the precursor ion envelope (to ensure capture of the maximum fraction of deuteriation) and unit resolution on the mass offsets for the selected fragment. Maximizing the transmission of deuteriation into the collision cell ensures that a given fragment is maximally deuteriated, and the high shift sensitivity is returned when the two isotopic selections of the fragment are well resolved.

In Method 2, Q1 is toggled between two offset  $m/z$  values representing the same precursor ion, but Q3 is fixed upon a  $m/z$  of a given fragment. Here, deuteriation of the precursor ion is measured,

as the fragment is simply a reporter for peptide signal. The simulations in Fig. 3C and D show relationships comparable to Method 1. High sensitivity to mass shifts is seen when the offset transmission windows are well separated, which can be achieved through a combination of larger offsets and higher resolution ion selection. Although the isotopic distribution of the fragment ion can change as a function of deuteriation, low resolution transmission in Q3 can be effective in transmitting the entire isotopic distribution. The resolution setting in Q3 could likely be reduced to “unit” with only a minor loss in shift sensitivity, however this was not explored.

For both methods, it is again interesting to note that optimal shift sensitivity is obtained under conditions of reduced %D incorporation. However, this arises simply because the  $m/z$  values for the transmission windows are based upon M and M+x values. The deuteriation range for optimum shift sensitivity would itself shift, in either method, if alternate window positions would be selected (e.g., M+y and M+x+y). However, as noted earlier, we prefer to select on the basis of the monoisotopic ion as these are known in any given experiment, whereas the y value would need to be determined experimentally.

#### 4.2. Validation with deuterated peptides

To test the validity of these simulations, we compared both methods of shift measurement against the conventional centroid determination approach, using linear ion trap data from the QTRAP 2000. Neurotensin was used under equilibrium conditions spanning 0–25% deuterium incorporation and centroid measurements were made with no correction for back exchange. As a measure of precision, we determined the error in the slope of the linear response (Fig. 4A) to be 3.6% relative standard deviation (RSD). This is a typical result for both the linear ion trap data and the higher resolution TOF data sets. Both methods were then applied to the same deuteriation range, using two common transition sets. The conditions were not optimized for maximum shift sensitivity, but rather were applied to determine the impact of method type on sensitivity. Here, both Method 1 and Method 2 were operated with low resolution selection on both quadrupoles, with 1 Th window offsets in the toggling quadrupole. Method 2 applied to a low mass fragment ( $m/z$  197,  $a_2$  ion) provides a shift sensitivity comparable to the conventional method, as shown in the error of the slope (3.3% RSD, see Fig. 4B). However, method selection and the transition set within a given method are clearly important. For example, as shown in Fig. 4B, applying Method 1 to the same low mass fragment is not sensitive. Conversely, when selecting the high mass fragment ion ( $m/z$  643,  $y_{10}$  ion), Method 1 outperforms Method 2.

To avoid bias, these relationships require evaluation on a larger set of peptides. However, we first sought to determine if MRM methods for shift measurement provided lower limits of detection and a wider dynamic range of measurement, compared to the conventional approach. This is a requirement for continued exploration of the concept. Table 1 demonstrates, for 20% deuterated neurotensin, that both Method 1 and Method 2 can be operated with high precision, comparable to that provided by conventional measurements. The benefit of the MRM approach is evident at the lower concentrations, where shift measurement precision is preserved over four orders of magnitude. Sample carryover in the fluidics system was the barrier to lower limits of detection. The

conventional MS approach was very sensitive to the quality of the isotopic distribution, and here is only reliable over two orders of magnitude in concentration (Table 1). This is further illustrated in Fig. 5, demonstrating the difference in signal quality at 40 nM peptide concentration for MRM Method 1 and the conventional detection strategy.

In the simple example of deuterated neurotensin, both Method 1 and Method 2 appear equally sensitive measures of mass shift, however the transition selection plot (Fig. 4B) suggests that this may not always be the case. A wider comparison of both methods was conducted, using a larger set of peptides selected from a complex pepsin digest of equilibrium deuterated  $\alpha/\beta$ -tubulin. This was done with a view to developing a useful set of guidelines for fragment selection and optimization of sensitivity. The set provides a typical range of mass and charge state arising from bottom-up H/D experiments, and presents a moderately complex chemical background (>200 peptides eluting over 6 min). For the nine peptides monitored, transitions were developed around the base peak in the corresponding MS/MS spectra. That is, both methods monitored the same fundamental transition (Table 2).

We first explored the effect of transmission window on the precision of shift measurement for the two methods. That is, the width of the offset windows in each method was varied between low and unit resolution. In general, Table 2 shows that higher resolution windows lead to measurements with higher precision, for both methods. Exceptions such as peptide 6 (Method 1) may arise from “edge effects”, when transmission windows bisect an isotopic peak. This can lead to heightened variability [18]. Although the same fundamental transition was selected, Table 2 shows that Method 2 slightly outperforms Method 1, but more properly suggests that each individual transition should be tailored for highest precision (for example, notice that peptide 1 is better treated by Method 1).

In evaluating this variability further, the resolution of the offset windows was fixed but the degree of the offset varied. This was conducted on the same set of peptides, but for Method 2 alone. Three representative peptides of the set are shown in Fig. 6. There is an

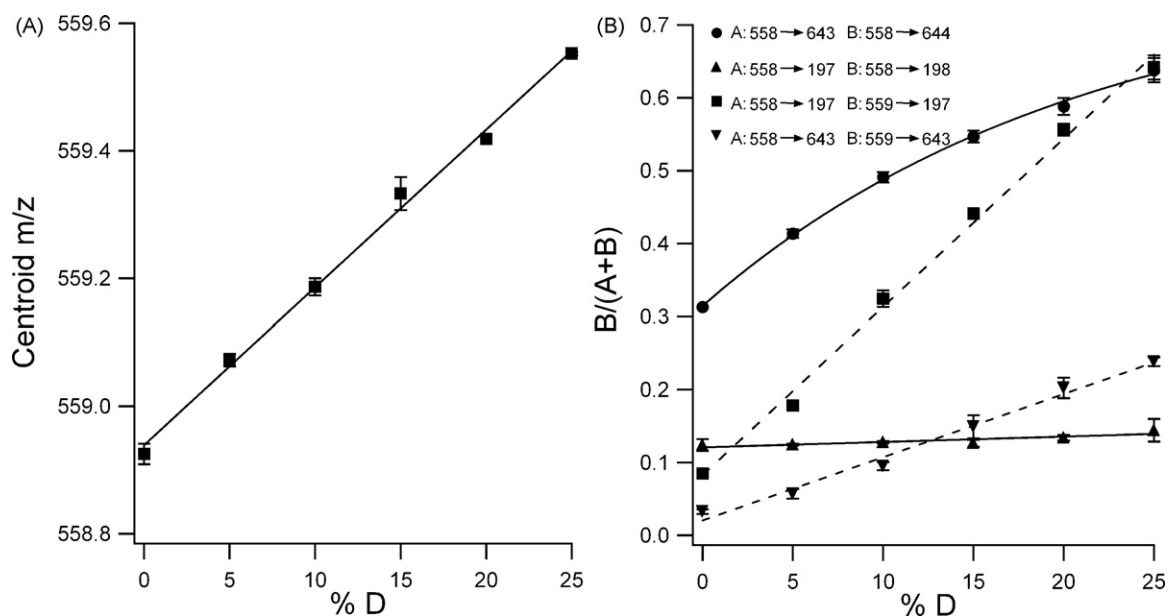


**Fig. 4.** Shift sensitivity for conventional and MRM-based methods. (A) Centroid  $m/z$  determined in the conventional fashion from linear ion trap data. (B) Fractional transition intensities based on both Method 1 and Method 2 approaches, for two fundamental transitions. Transitions in the legend represent Method 1 (filled circle and filled triangle, fitted with solid lines) and Method 2 (filled square and filled inverted triangle, fitted with dashed lines). Data presented as averages of replicate injections for the peptide neurotensin,  $\pm$ one standard deviation. The 3+ charge state ( $m/z$  558) was monitored, and either the  $y_{10}$  fragment ( $m/z$  643) or the  $a_2$  fragment ( $m/z$  197). Data uncorrected for back exchange.

**Table 1**  
Comparison of methods for shift measurement precision and dynamic range.

[NT] <sup>a</sup>	MRM Method 1		MRM Method 2		LIT mode			
	$\Delta (M, M+2)^b$	%RSD	$\Delta (M, M+4)^c$	%RSD	$\Delta (M, M+3)^d$	%RSD	$\Delta D^e$	%RSD
2.5	0.17	6.1	0.37	1.9	0.17	8.8	–	–
9.8	0.18	7.5	0.37	9.1	0.13	11.1	–	–
39	0.20	5.8	0.45	3.1	0.16	2.7	0.44	9.2
156	0.19	2.9	0.43	3.2	0.16	2.7	0.40	7.8
625	0.19	3.0	0.46	1.7	0.17	5.8	0.45	3.4
2500	0.20	1.8	0.43	3.7	0.17	3.1	0.45	3.2
10,000	0.19	1.4	0.39	1.4	0.16	5.0	0.39	0.5

<sup>a</sup> Concentration of neurotensin in nM (2  $\mu$ L injected) equilibrated in 20% D<sub>2</sub>O.

<sup>b</sup> Fractional transition intensities  $B/(A+B)$ , where A is 558  $\rightarrow$  643 and B is 558  $\rightarrow$  644. Corrected for non-deuterated fractional transition intensities.

<sup>c</sup> As b, where A is 558  $\rightarrow$  643 and B is 558  $\rightarrow$  645.

<sup>d</sup> As b, where A is 558  $\rightarrow$  197 and B is 559  $\rightarrow$  197.

<sup>e</sup> Centroid value for  $m/z$  558.00–560.88. Values corrected for non-deuterated centroid value.

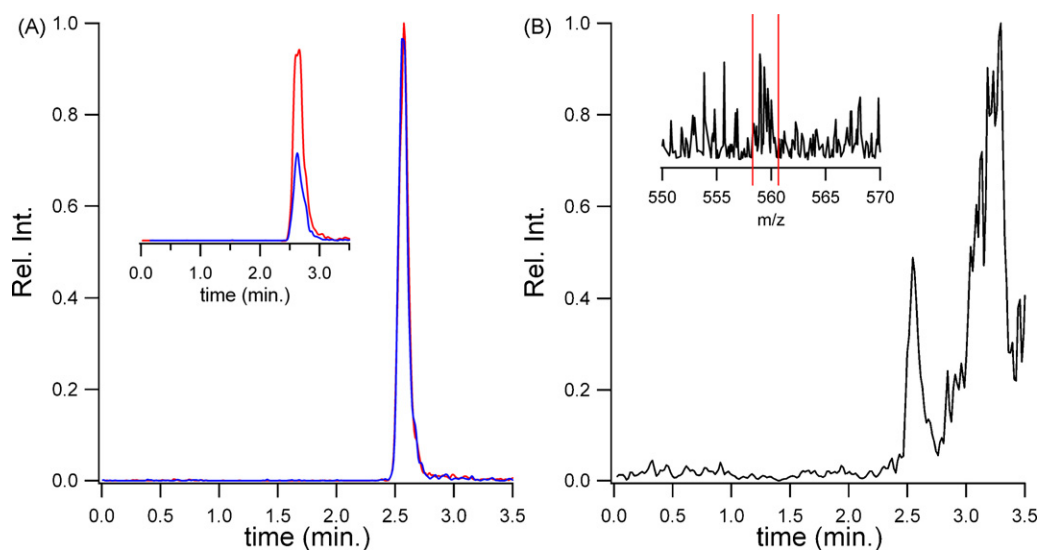


**Fig. 5.** Detection sensitivity of shift measurements, using an MRM method and the conventional approach. (A) Application of Method 1 to an injection of 20% deuterated 40 nM neurotensin, showing extracted ion chromatograms for transitions 558  $\rightarrow$  643 (red) and 558  $\rightarrow$  644 (blue). Inset represents an unlabeled control. All transitions monitored at “low” resolution. (b) Application of the conventional method to the same solution, showing an extracted ion chromatogram for the  $m/z$  range highlighted between red bars (inset, representing average spectrum over the chromatographic peak at 2.6 min.). (For interpretation of the references to color in this figure legend, the reader is referred to the web version of the article.)

**Table 2**  
Optimization of shift precision for MRM methods.

Peptide sequence	Residues	Charge	Method 1 <sup>a,b</sup>		Method 2 <sup>a,c</sup>	
			Low/low	Low/unit	Low/low	Unit/low
1. FSVMPSPKVSD	167–177	2	5.8	4.1	18.8	15.8
2. FSVVSPKVSdT	167–178	2	9.1	13.3	15.0	6.6
3. ATMSGVTTSLRFPGQL	231–246	2	26.8	6.6	5.4	1.9
4. LYRGDVVPKDVNA	318–330	2	20.5	6.1	24.0	4.2
5. YRGDVVPKDVNA	319–330	2	21.6	5.9	25.6	5.9
6. FVEWIPNNVKVAV	341–353	2	10.0	33.4	14.5	4.9
7. FVDWCPTGF	343–351	1	24.6	23.6	11.5	9.8
8. VDWCPPTGF	344–351	1	10.2	13.7	23.1	11.5
9. KVGINYQPPTVPPGGDL	352–368	2	8.0	3.1	9.1	6.9

<sup>a</sup> Fractional intensity  $B/(A+B)$  corrected with non-deuterated transition data, with error representing propagated %RSD.

<sup>b</sup> Fractional intensity calculated using M and M+2 peaks in the product ion isotopic distribution (all product ions singly charged).

<sup>c</sup> Fractional intensities calculated using the M and M+2 peaks for singly charged product ions and M and M+4 peaks for doubly charged products.

optimum offset for each peptide ranging between 1 and 3 Th, which reflects charge state, peptide  $m/z$  and the peptide deuterium level. For example, large singly charged peptides with high deuteration would require a larger offset than a small doubly charged peptide with low deuteration. Here as well, optimization of this parameter is simplified using lower % D<sub>2</sub>O. Note that the apparent reduction in shift precision at high offsets for LYRGDVVPKDVNA is anomalous,

as the width of the deuterated isotopic envelope was exceeded by the high mass transmission window.

#### 4.3. Mass shift perturbation detection by MRM

Ultimately, a new method for shift detection should be tested against conventional methods for its ability to detect an induced

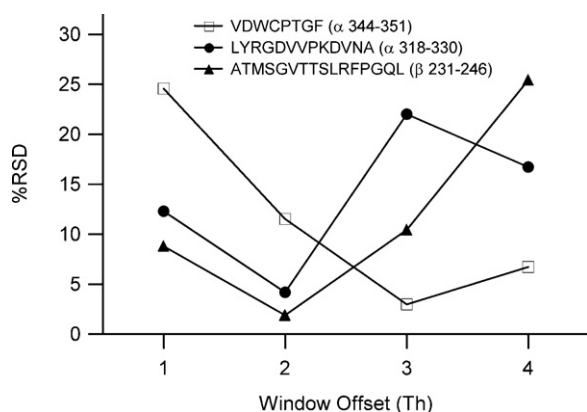


**Fig. 6.** Impact of window offsets on shift measurement precision. Select peptides from  $\alpha/\beta$ -tubulin digest showing the influence of progressively larger spacing between offset windows in Q1, for Method 2 operation. Offset spacing expressed in Th, with precision expressed as %RSD arising from replicate measurements.

structural change in a protein. To this end, we conducted a drug binding study to profile the effect of two different classes of ligand on  $\alpha/\beta$ -tubulin, an important anticancer drug target. Drugs based upon taxol, a natural product isolated from the Pacific

yew tree, bind and stabilize the polymerized form of  $\alpha/\beta$ -tubulin (microtubules). Conversely, drugs derived from the vinca alkaloids, natural products isolated from the periwinkle, bind to the free dimer and inhibit normal microtubule formation. Although these mechanisms are different, both drugs arrest cells in mitosis and eventually induce cell death. It has been shown previously that ligands binding to the taxol binding site induce extensive stability throughout the protein, resulting from significant changes to structure and dynamics in the polymerized state [19,21]. Conversely, the vinca alkaloids induce a relatively subtle change, highlighting a binding site that appears to bridge two dimers (manuscript in preparation). We established a targeted MRM assay for the two binding sites and key areas of the protein sensitive to assembly. The set of peptides listed in Table 2 represent these regions. A conventional bottom-up approach was applied to the measurement of the mass shift, using higher resolution MS data from the QSTAR platform (Fig. 7A). This data shows that docetaxel reduces mass shifts across all peptides in the set as expected, since this is a potent taxol mimetic [22]. Conversely, vinblastine reduces mass shifts exclusively in areas related to its binding site [23], but not in areas typically stabilized upon microtubule assembly. Fig. 7B shows that an optimized MRM shift assay faithfully renders these mass shifts and appears more discriminating than the conventional method (see Supplementary Table 1 for optimized MRM parameters).

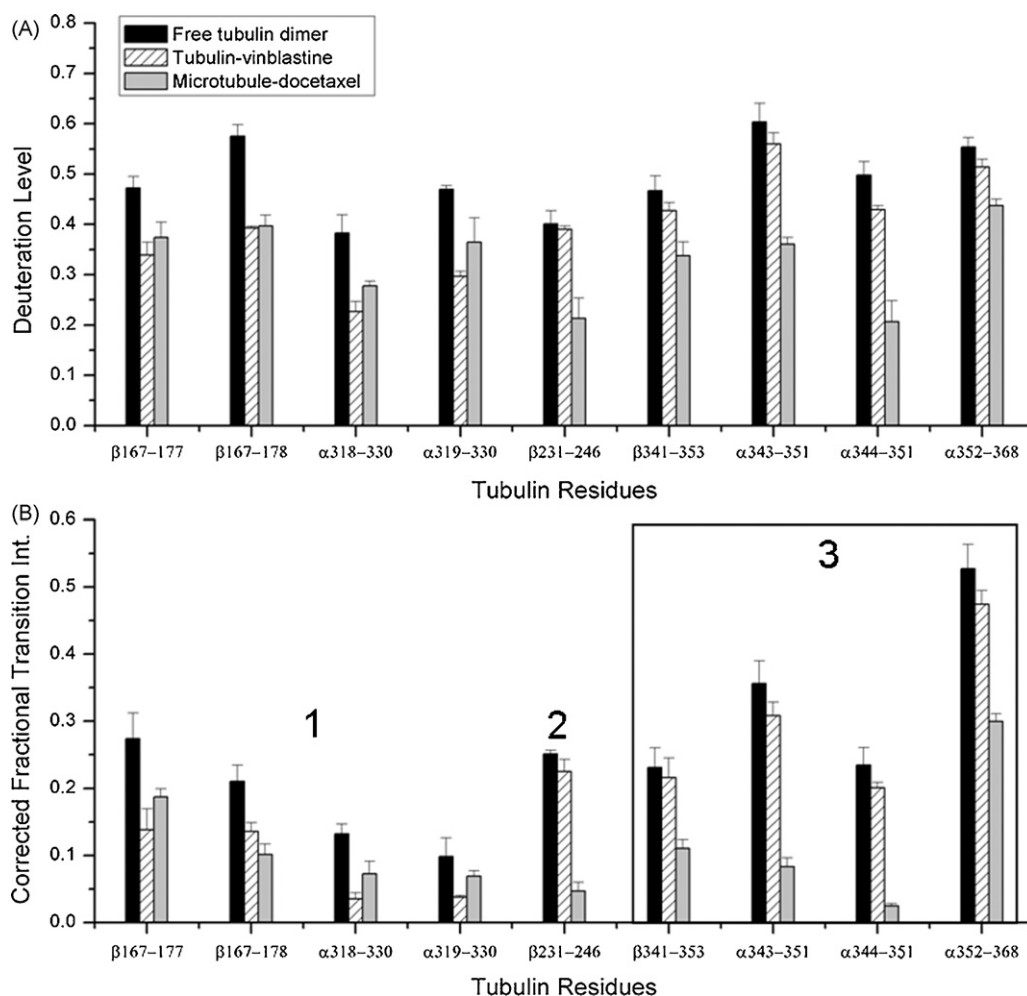


**Fig. 7.** Sensing key regions in drug-treated  $\alpha/\beta$ -tubulin with the MRM method. (A) Conventional mapping of mass shifts using higher resolution QSTAR data for a select set of peptides (B) Optimized MRM assay for the same set of peptides, based upon Method 2 operation. Numbered regions represent the vinblastine binding site (1), the docetaxel binding site (2) and polymerization contacts (3). Error bars represent one standard deviation. The deuterium level (A) and the fractional transition intensity (B) are referenced against the undeuterated control.



#### 4.4. MRM optimization guidelines

The simulations and empirical data arising from both neurtensin and  $\alpha/\beta$ -tubulin suggest a set of guidelines that should be followed when optimizing an MRM shift assay.

##### 4.4.1. Peptides for Method 1 should have their entire envelope mass selected in Q1

While the envelopes can be truncated, this will reduce shift sensitivity. Therefore, when considering charge state selection, higher charge states may be preferred because the ion selection window can be compressed. This will generally aid in reducing noise in the transition being monitored. As with proteomics application, selecting a 2+ charge state will generally provide the richest set of fragments for transition selection.

##### 4.4.2. Transitions for Method 1 should be drawn from high mass fragments

Low mass fragments, as shown in Fig. 4B, only offer a small number of deuteration sites. For example, the  $a_2$  ion ( $m/z$  197) possesses only 10% of the deuteration sites seen in the precursor. Since Method 1 is based upon deuterium detection in the fragments, low mass fragments are disadvantaged.

##### 4.4.3. Transition selection for Method 1 may be influenced by scrambling

Because the deuteration measurement is applied to fragment ions, nonuniform gas-phase deuterium scrambling could influence the utility of one fragment over another. High energy ion desolvation and/or fragmentation conditions will ensure extensive scrambling in CID-based measurements, but exceptions have been known to occur. In the extreme, a fragment could be selected that does not adequately represent the full length peptide. Conversely, this could be an advantage for experiments where deuterium localization requires sensitive monitoring.

##### 4.4.4. Peptides for Method 2 should be sampled in Q1 at unit resolution

While a lower resolution setting can be used for the offset transmission windows, unit resolution permits good separation of the offsets. At the same time it permits the use of narrow deuteration ranges. This has substantial analytical benefit, as has been shown previously [16]. Ion selection can therefore be restricted to the natural isotopic envelope, which will help to reduce any differences in the noise levels between the transition offsets. This differential noise level is a primary reason to avoid the use of higher deuteration levels.

##### 4.4.5. Transitions for Method 2 can be selected from any fragment

This allows for fragment selection on the basis of favorable analytical characteristics (e.g., maximum S/N), since Method 2 is not influenced by deuterium scrambling. High mass fragments have wider isotopic envelopes, requiring a wider transmission window in Q3. Lower mass fragments could be sampled with a smaller transmission window. As a result, low mass fragments may have a slight advantage over higher mass fragments. However, this must be balanced by the lower noise levels often found with transitions based on higher mass fragments.

Given the number of peptides that might be enrolled into an MRM-based shift monitoring experiment, rigorous optimization of the %RSD has the potential to be time consuming. Overall, we suggest that an MRM strategy based on Method 2, involving unit resolution sampling in Q1 with a minimum offset value of 1 Th, provides the best general conditions for high shift sensitivity. This can be supplemented by Method 1 in situations where the noise

characteristics of Method 2 are unfavorable. In our lab, an efficient optimization strategy involves analysis of digests equilibrated with (e.g., 25%) and without D<sub>2</sub>O. Method 2 is used first, with two or three candidate fragments selected from the initial peptide indexing experiment (i.e., tandem MS peptide identification data). The best individual transition is selected from runs of the non-deuterated digest, which are processed under conventional H/DX-MS conditions (i.e., cold chromatography, shorter gradients). The greatest attrition occurs at this stage. A two-point measure of sensitivity is then conducted, using replicate analysis of the deuterated digest and non-deuterated digest. Suboptimal %RSD values in a subset of the peptides trigger a shift in the size of the window offset and reanalysis in both Method 2 and Method 1, for final transition selection. These routines can be readily managed with an autosampler-based system, requiring a couple of days for optimizing the shift assay for a modest set of peptides (<40).

## 5. Conclusions

This MRM approach to shift measurement offers several advantages. In the first place, the increased dynamic range should support improved sequence coverage obtained by pepsin digests. Often, peptides that were sequenced effectively under conventional LC/MS conditions are harder to detect under the constraints of an H/DX-MS experiment (fast separations, cold chromatography). The MRM approach should retain high sequence coverage, and with a scheduled MRM mode of operation, could accommodate all peptides in a digest. Second, this increased dynamic range may permit a further compression of chromatographic run time. Although limited by the number of transitions that could be monitored per unit time, smaller protein systems could be processed under “ballistic” chromatographic conditions [24,25]. Third, H/D data analysis is simplified. Mass shift measurement is reduced to the ratio of transition intensities, which conventional reporting tools for triple quadrupole instruments are designed to generate. From the applications perspective, many high throughput H/DX-MS experiments only require monitoring select peptides (e.g., drug-lead evaluation). The MRM shift measurement strategy will promote targeted assays and combined with simplicity in operation and data analysis, will enable higher throughput applications.

## Acknowledgements

This research was funded in part by the Natural Sciences and Engineering Research Council of Canada, the Canadian Institutes for Health Research, Canada Foundation for Innovation and the Canada Research Chair program. We are grateful to Dan L. Sackett (Laboratory of Integrative and Medical Biophysics, National Institute of Child Health and Human Development, Bethesda, MD, USA) for the gift of vinblastine.

## Appendix A. Supplementary data

Supplementary data associated with this article can be found, in the online version, at doi:10.1016/j.ijms.2010.07.008.

## References

- [1] V. Chevelkov, Y. Xue, D.K. Rao, J.D. Forman-Kay, N.R. Skrynnikov, N-15(H/D)-SOLEXPY experiment for accurate measurement of amide solvent exchange rates: application to denatured drkN SH3, *J. Biomol. NMR* 46 (2010) 227–244.
- [2] H.J. Dyson, M. Kostic, J. Liu, M.A. Martinez-Yamout, Hydrogen–deuterium exchange strategy for delineation of contact sites in protein complexes, *FEBS Lett.* 582 (2008) 1495–1500.
- [3] M.J. Chalmers, S.A. Busby, B.D. Pascal, Y.J. He, C.L. Hendrickson, A.G. Marshall, P.R. Griffin, Probing protein ligand interactions by automated hydrogen/deuterium exchange mass spectrometry, *Anal. Chem.* 78 (2006) 1005–1014.

- [4] S.Y. Dai, T.P. Burris, J.A. Dodge, C. Montrose-Rafizadeh, Y. Wang, B.D. Pascal, M.J. Chalmers, P.R. Griffin, Unique ligand binding patterns between estrogen receptor alpha and beta revealed by hydrogen–deuterium exchange, *Biochemistry* 48 (2009) 9668–9676.
- [5] X. Zhang, E.Y.T. Chien, M.J. Chalmers, B.D. Pascal, J. Gatchalian, R.C. Stevens, P.R. Griffin, Dynamics of the beta(2)-adrenergic G-protein coupled receptor revealed by hydrogen–deuterium exchange, *Anal. Chem.* 82 (2010) 1100–1108.
- [6] M.J. Bennett, J.K. Chik, G.W. Slys, T. Luchko, J. Tuszynski, D.L. Sackett, D.C. Schriemer, Structural mass spectrometry of the alpha beta-tubulin dimer supports a revised model of microtubule assembly, *Biochemistry* 48 (2009) 4858–4870.
- [7] M.J. Bennett, K. Barakat, J.T. Huzil, J. Tuszynski, D.C. Schriemer, Discovery and characterization of the laulimalide-microtubule binding mode by mass shift perturbation mapping, *Chem. Biol.*, in press.
- [8] E.R. Zuiderweg, Mapping protein–protein interactions in solution by NMR spectroscopy, *Biochemistry* 41 (2002) 1–7.
- [9] J. Stark, R. Powers, Rapid protein–ligand costructures using chemical shift perturbations, *J. Am. Chem. Soc.* 130 (2008) 535–545.
- [10] Y.W. Bai, J.S. Milne, L. Mayne, S.W. Englander, Primary structure effects on peptide group hydrogen-exchange, *Proteins: Struct. Funct. Genet.* 17 (1993) 75–86.
- [11] G.P. Connelly, Y.W. Bai, M.F. Jeng, S.W. Englander, Isotope effects in peptide group hydrogen-exchange, *Proteins: Struct. Funct. Genet.* 17 (1993) 87–92.
- [12] S.W. Englander, Hydrogen exchange and mass spectrometry: a historical perspective, *J. Am. Soc. Mass Spectrom.* 17 (2006) 1481–1489.
- [13] H.M. Zhang, G.M. Bou-Assaf, M.R. Emmett, A.G. Marshall, Fast reversed-phase liquid chromatography to reduce back exchange and increase throughput in H/D exchange monitored by FT-ICR mass spectrometry, *J. Am. Soc. Mass Spectrom.* 20 (2009) 520–524.
- [14] S. Kazazic, H.M. Zhang, T.M. Schaub, M.R. Emmett, C.L. Hendrickson, G.T. Blakney, A.G. Marshall, Automated data reduction for hydrogen/deuterium exchange experiments, enabled by high-resolution Fourier transform ion cyclotron resonance mass spectrometry, *J. Am. Soc. Mass Spectrom.* 21 (2010) 550–558.
- [15] G.M. Bou-Assaf, J.E. Chamoun, M.R. Emmett, P.G. Fajer, A.G. Marshall, Advantages of isotopic depletion of proteins for hydrogen/deuterium exchange experiments monitored by mass spectrometry, *Anal. Chem.* 82 (2010) 3293–3299.
- [16] G.W. Slys, A.J. Percy, D.C. Schriemer, Restraining expansion of the peak envelope in H/D exchange-MS and its application in detecting perturbations of protein structure/dynamics, *Anal. Chem.* 80 (2008) 7004–7011.
- [17] A.J. Percy, G.W. Slys, D.C. Schriemer, Surrogate H/D detection strategy for protein conformational analysis using MS/MS data, *Anal. Chem.* 81 (2009) 7900–7907.
- [18] P.H. Dawson, *Quadrupole Mass Spectrometry and its Applications*, AIP Press, Woodbury, NY, 1995.
- [19] J.T. Huzil, J.K. Chik, G.W. Slys, H. Freedman, J. Tuszynski, R.E. Taylor, D.L. Sackett, D.C. Schriemer, A unique mode of microtubule stabilization induced by peloruside A, *J. Mol. Biol.* 378 (2008) 1016–1030.
- [20] G.W. Slys, C.A. Baker, B.M. Bozsa, A. Dang, A.J. Percy, M. Bennett, D.C. Schriemer, Hydra: software for tailored processing of H/D exchange data from MS or tandem MS analyses, *BMC Bioinformatics* 10 (2009) 162–175.
- [21] H. Xiao, P. Verdier-Pinard, N. Fernandez-Fuentes, B. Burd, R. Angeletti, A. Fiser, S.B. Horwitz, G.A. Orr, Insights into the mechanism of microtubule stabilization by Taxol, *Proc. Natl. Acad. Sci. U.S.A.* 103 (2006) 10166–10173.
- [22] M.T. Huizing, V.H.S. Misser, R.C. Pieters, W.W.T. Huinink, C.H.N. Veenhof, J.B. Vermorken, H.M. Pinedo, J.H. Beijnen, Taxanes—a new class of antitumor agents, *Cancer Invest.* 13 (1995) 381–404.
- [23] B. Gigant, C.G. Wang, R.B.G. Ravelli, F. Roussi, M.O. Steinmetz, P.A. Curmi, A. Sobel, M. Knossow, Structural basis for the regulation of tubulin by vinblastine, *Nature* 435 (2005) 519–522.
- [24] A.C. Li, M.A. Gohdes, W.Z. Shou, 'N-in-one' strategy for metabolite identification using a liquid chromatography/hybrid triple quadrupole linear ion trap instrument using multiple dependent product ion scans triggered with full mass scan, *Rapid Commun. Mass Spectrom.* 21 (2007) 1421–1430.
- [25] C. De Nardi, F. Bonelli, Moving from fast to ballistic gradient in liquid chromatography/tandem mass spectrometry pharmaceutical bioanalysis: matrix effect and chromatographic evaluations, *Rapid Commun. Mass Spectrom.* 20 (2006) 2709–2716.